Valence-skipping and negative-U in the d-band from repulsive local Coulomb interaction

Hugo U. R. Strand*
University of Fribourg, CH-1700 Fribourg, Switzerland and University of Gothenburg, SE-412 96 Gothenburg, Sweden

We show that repulsive local Coulomb interaction alone can drive valence-skipping charge disproportionation in the degenerate d-band, resulting in effective negative-U. This effect is shown to originate from anisotropic orbital-multipole scattering, and it occurs only for d^1, d^4, d^6, and d^9 fillings (and their immediate surroundings). Explicit boundaries for valence-skipping are derived, and the paramagnetic phase diagram for d^4 and d^6 is calculated. We also establish that the valence-skipping metal is very different, in terms of its local valence distribution, compared to the atomiclike Hund's metal. These findings explain why transition-metal compounds with the aforementioned d-band fillings are more prone to valence-skipping charge order and anomalous superconductivity.

I. INTRODUCTION

Some elements in the Periodic Table have a strong tendency to occur only in certain valence states when compounded. Whenever one particular intermediate valence state is very rare or completely missing, the corresponding element is denoted as valence-skipping. The most prominent examples are the post-transition metals, Tl, Bi, Sb, etc., which display missing valences in many of their compounds [1]. In general, valence-skipping is driven by a negative effective Coulomb repulsion U_{eff}, but the mechanism causing this is debated. Anderson [2] showed that static lattice relaxation can drive $U_{\text{eff}} < 0$. However, Varma [1] noted that even free atoms have reduced U_{eff} in the unfavorable valences, and he proposed an intra-atomic electronic mechanism. More recently, the electronic route has been discredited for these elements in favor of the lattice relaxation mechanism [3].

Apart from the post-transition metals, valence-skipping has also been observed in transition metals [1] with a $d^n \to d^{n-1} + d^{n+1}$ type of charge disproportionation. Experimentally, the most evident examples are the iron compounds (La,Ca)FeO_3 [4,5], (La,Sr)FeO_3 [5,6], and $Sr_3Fe_2O_7$ [7], where Mössbauer spectroscopy has established valence-skipping $Fe^{4+} \to Fe^{3+} + Fe^{5+}$, ($d^4 \to d^3 + d^5$) charge-order, even in the absence of lattice relaxation [4,7]. Theoretically, Katayama-Yoshida and Zunger [8] showed that effective monopole screening of intra-atomic interactions indeed can give rise to $U_{\text{eff}} < 0$ in transition-metal impurities. This idea has been used to explain the charge-order in $YNiO_3$ within a two-band e_g model [9]. But the complete d-band still deserves more attention.

The fact that some authors even refer to valence-skipping as "mysterious" [10,11] shows the need for better understanding of the underlying mechanism behind this phenomenon and its systematics. The resulting negative-U model, however, has been studied extensively and shown to drive both charge-order and anomalous superconductivity [12]. So unveiling the mysteries of valence-skipping could pave the way for more exotic physics.

In this article, we show that the higher orbital-multipole part of the repulsive intra-atomic Coulomb interaction alone can drive valence-skipping in the degenerate d-band. This effect is found to be limited to the particular fillings d^1, d^4, d^6, and d^9, and their immediate surroundings. From a multiplet analysis, we derive explicit bounds for valence-skipping, and finally the emerging anomalous valence fluctuations in the paramagnetic metal are studied. We note and discuss the correlation of the orbital-multipole active fillings in the compounded transition metals with experimental results for (i) charge disproportionation in d^1: V^{4+}, d^4: Fe^{4+}, Mn^{3+}, d^6: Co^{3+}, and d^9: Au^{2+}, and (ii) anomalous super conductivity in d^4: Ru^{4+}, d^6: Fe^{2+}, and d^9: Cu^{2+}.

II. MODEL

Let us begin by constructing a minimal model for the correlated d-band. We assume that the Coulomb interaction is local and rotationally invariant, a good first approximation for transition metals [13]. Under this assumption, the interaction is exactly given by the Slater-Condon angular-momentum expansion, and the Slater integrals $F^{(0)}$, $F^{(2)}$, and $F^{(4)}$ [14]. For the electron hopping, we use a degenerate semicircular density of states, and we take the half-bandwidth as our unit of energy.

In general, the local interaction describes electron-pair scattering between local two-particle states, and rotational invariance ensures that these processes conserve local total orbital momentum L and total spin S. As we are going to see, anisotropic orbital-multipole scattering (i.e., for $L > 0$) has an intrinsic connection to valence-skipping. To make this clear, we now seek to isolate this contribution to the interaction.

Within the Slater-Condon interaction, the $F^{(0)}$ term is a density-density interaction with isotropic scattering, while the $F^{(2)}$ and $F^{(4)}$ terms have different scattering strengths for all L and S. Interestingly, their orbital-multipole anisotropies cancel out when $F^{(4)}/F^{(2)} = 9/5$. This corresponds to a Laporte-Platt degenerate point of the Slater-Condon interaction with large accidental degeneracies of multiplets [15].

Spurred by this observation, we investigated the Slater-Condon interaction in detail [16], and we found that in this point it simplifies to the rotationally invariant Kanamori interaction [17], having the compact form

$$\hat{H} = (U - 3J)\hat{N}(\hat{N} - 1)/2 + J(\hat{Q}^2 - \hat{S}^2), \qquad (1)$$

*hugo.strand@unifr.ch

where $\hat{N}$ is the total number operator, and $\hat{S}^2$ and $\hat{Q}^2$ are the total spin and quasispin operators [14].

The Kanamori interaction and the roles of its coupling parameters, the Hubbard U, and Hund's rule J have already been studied extensively [18]. This makes the reduction of the Slater-Condon interaction (at the Laporte-Platt degenerate point $F^{(4)}/F^{(2)} = 9/5$) very interesting. At this point, U and J alone can be used to determine $F^{(k)}$.

But let us first establish our claim that anisotropic orbital-multipole scattering is indeed missing in Eq. (1). We need not worry about the density-density interaction giving isotropic scattering (like the $F^{(0)}$ term). So all nontrivial scattering in Eq. (1) stems from $J(\hat{Q}^2 - \hat{S}^2)$, where $\hat{S}^2$ (acting in spin space) does not differentiate between orbital angular-momentum channels L directly. The quasispin operator $\hat{Q}^2$, however, does differentiate in L, but it scatters only in the monopole channel ($L = 0$) [14]. This proves our point that the Slater-Condon interaction, at the Laporte-Platt degenerate point $F^{(4)}/F^{(2)} = 9/5$, is free from anisotropic orbital-multipole interactions. Hereafter we will refer to these interactions as simply "multipole interactions."

Guided by our findings, we propose the following reparametrization of the Slater-Condon interaction:

$$F^{(0)} = U - \frac{8}{5}J, \quad F^{(2)} = 49\left(\frac{1}{\gamma} + \frac{1}{7}\right)J, \quad F^{(4)} = \frac{63}{5}J, \quad (2)$$

using U, J, and $1/\gamma$, where $1/\gamma$ controls the relative strength of the multipole interactions. A cautionary remark is needed: the multipole parametrization is arbitrary (Ref. [19] uses another equivalent form), and the choice of $1/\gamma$ in Eq. (2) is a matter of taste. [Our choice is motivated by the simple form Eq. (2) takes in terms of the Racah parameters, $A = U - 3J$, $B = J/\gamma$, and $C = J$.] However, the Kanamori limit, without multipole terms, is well defined by $1/\gamma = 0$. In what follows, we set $1/\gamma = 1/4$, which corresponds to $F^{(4)}/F^{(2)} \approx 0.65$, in the relevant regime for the transition metals [20].

III. ATOMIC ENSEMBLE LIMIT

We are now in a position to start our study of the d-band model. Much can in fact be learned in the limit of strong interactions, where the system turns in to an ensemble of isolated atoms with known N-electron ground-state energies E_N [14,21,22]. For the ensemble with integer average filling n, the obvious ground-state candidate is the homogeneous state with energy E_n. But there is also the possibility of phase-separated mixtures of atomic states with N_1 and N_2 electrons. In general, such a mixture has the energy $E^{(n)}_{N_1,N_2} = E_{N_1} + (E_{N_2} - E_{N_1})(n - N_1)/(N_2 - N_1)$ assuming $N_1 < n < N_2$.

We have compared all candidate states for every integer n and located the ground-state crossings as a function of J/U and $1/\gamma$; see Fig. 1 for an example. We find that (as in Fig. 1) the valence-skipping $d^{n-1} + d^{n+1}$ state is the ensemble ground state in the range $j_{d1} < J/U < j_{d2}$, with $1/\gamma$-dependent bounds $j_{d1} = 1/(3 + 8/\gamma)$ and $j_{d2} = 1/(3 + 2/\gamma)$, but only for $n = 1$, 4, 6, and 9. For the other integer n, the $d^{n-1} + d^{n+1}$ state never becomes the ground state. When $J/U > j_{d2}$, the ensemble has a valence-split type of ground state for all n,

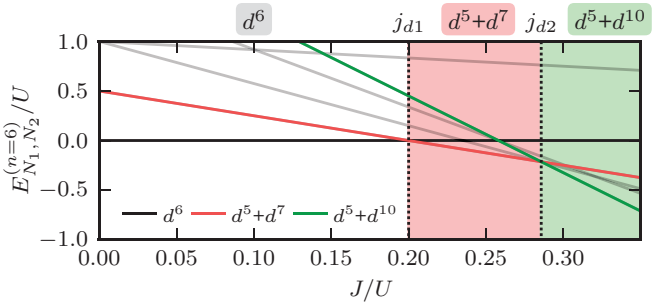

FIG. 1. (Color online) Ensemble energies as a function of J/U for all mixed-valence states (gray lines) relative to the atomic d^6 ground state (black line) for $1/\gamma = 1/4$. The energy crossings j_{d1} and j_{d2} (dotted lines) into the $d^5 + d^7$ valence-skipping (red line) and $d^5 + d^{10}$ valence-split (green line) phases are indicated.

composed by $d^0 + d^5$ for $n < 5$ and $d^5 + d^{10}$ for $n > 5$ (as in Fig. 1). The final phase diagram is shown in Fig. 2. Due to the growing importance of nonlocal interactions at high polarization, we refer to Appendix B for a separate discussion of the valence-split states.

With this background, we can understand the connection between valence-skipping and effective negative-U. The effective Hubbard repulsion U_{eff} is given by [8]

$$U_{\text{eff}} = E_{n+1} + E_{n-1} - 2E_n = 2\left(E^{(n)}_{n-1,n+1} - E_n\right), \quad (3)$$

and $U_{\text{eff}} < 0$ occurs only for concave series E_{n-1}, E_n, E_{n+1}. In the case of a valence-skipping ensemble ground state $d^{n-1} + d^{n+1}$, we are guaranteed that $E^{(n)}_{n-1,n+1} < E_n$, and Eq. (3) directly gives $U_{\text{eff}} < 0$.

But what is now the role of the multipole interactions? From the ensemble-phase diagram (Fig. 2), it is clear that the multipole interaction strength $1/\gamma$ directly controls the extent of the valence-skipping phase, and in the limit $1/\gamma \to 0$ this phase disappears. We conclude that the valence-skipping ground state is realized by the multipole interactions.

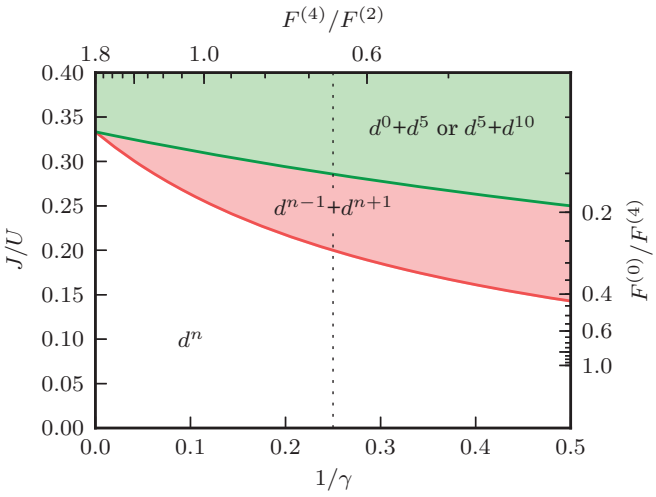

FIG. 2. (Color online) Ensemble phase diagram in the (J/U, $1/\gamma$) and ($F^{(4)}/F^{(2)}$, $F^{(0)}/F^{(4)}$) plane for integer average fillings n. The valence-skipping $d^{n-1} + d^{n+1}$ phase is only present for $n = 1, 4$, 6, and 9. The dotted line corresponds to $1/\gamma = 1/4$.

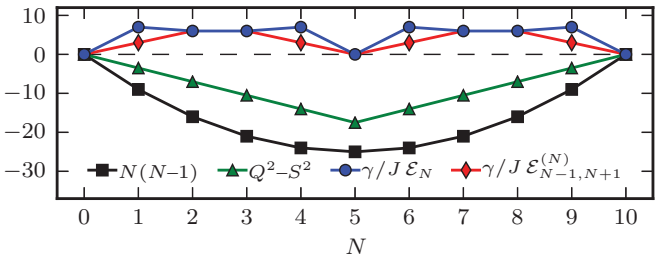

FIG. 3. (Color online) Atomic ground-state energy contributions for all N-electron fillings: density-density (squares), spin and quasispin scattering (triangles), and the multipole energies $\mathcal{E}_N$ (circles), up to (irrelevant) linear shifts μN. Note that only $\mathcal{E}_N$ is locally concave, and only for $N = 1, 4, 6$, and 9, where the valence-skipping state has a lower multipole contribution $\mathcal{E}^{(N)}_{N-1,N+1} = (\mathcal{E}_{N-1} + \mathcal{E}_{N+1})/2$ (diamonds).

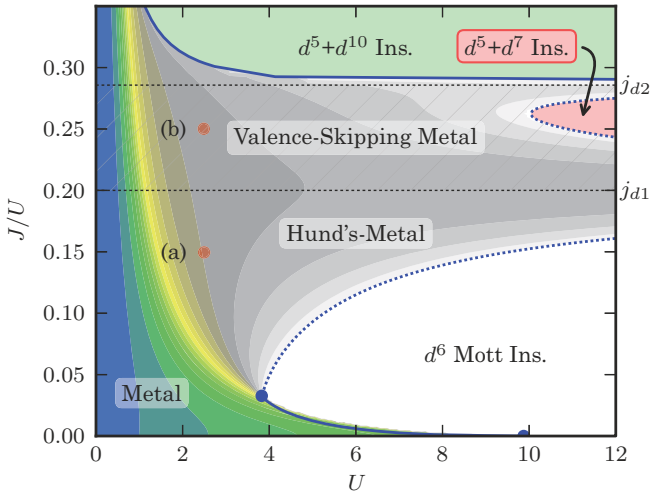

FIG. 4. (Color online) Phase diagram for d^6, with $1/\gamma = 1/4$, showing the contours of the local entanglement entropy of the metallic state, and the metal-insulator phase boundaries (blue lines); first- and second-order transitions are indicated (solid and dotted lines, respectively).

To understand why the effect is limited to only certain fillings, we decompose the atomic ground-state energies E_n in Kanamori and multipole contributions. As seen in Fig. 3, the isotropic and monopole terms are convex (as long as $U - 3J > 0$). However, the multipole energy $\mathcal{E}_N = E_N - (U - 3J)N(N-1)/2 - J(\langle \hat{Q}^2 \rangle - \langle \hat{S}^2 \rangle)$ is locally concave, but only for the special fillings $N = 1,4,6,9$, and it can therefore give $U_{\text{eff}} < 0$ for sufficiently large J/γ. Because of this, we will henceforth denote these fillings as "multipole-active." Further, using the fact that $E^{(N)}_{N-1,N+1} < E_N$ in the valence-skipping interaction regime for all multipole-active fillings N, one can directly show that $E^{(n)}_{N-1,N+1} < E^{(n)}_{N\pm1,N}$ for $N \lessgtr n \lessgtr N \pm 1$. Thus in the immediate surroundings of each multipole-active filling N, an ensemble with average filling n in the range $N - 1 < n < N + 1$ also has a valence-skipping ground state with energy $E^{(n)}_{N-1,N+1}$.

Let us close the discussion of the ensemble by recasting the valence-skipping criteria $J/U > j_{d1}$ in terms of $F^{(k)}$,

$$\frac{F^{(4)}}{F^{(2)}} \frac{\frac{F^{(0)}}{F^{(4)}} - \frac{1}{9}}{\frac{9}{5} - \frac{F^{(4)}}{F^{(2)}}} < \frac{40}{441}. \tag{4}$$

As $F^{(4)}/F^{(2)}$ varies weakly within the transition metals, fulfillment of Eq. (4) is mainly driven by ligand-induced effective monopole screening of $F^{(0)}$ [8].

IV. LATTICE MODEL

With these insights, we leave the subject of the strong-coupling limit and consider the full model with its competition between itineracy and local interactions. The ground state is calculated using the variational Gutzwiller method [23–25], previously shown to give phase diagrams in qualitative agreement with dynamical mean-field theory [26]. We limit the discussion to translationally invariant paramagnetic wave functions, employing the most general variational ansatz with the symmetry of our model.

Here we report results for d^6 (particle-hole symmetric to d^4), whose phase boundaries are shown in Fig. 4, together with the local entanglement entropy (defined as the von Neumann entropy $S = -\text{Tr}[\hat{\rho} \ln \hat{\rho}]$ of the site local many-body density matrix $\hat{\rho}$) contours of the metal [27]. The low J/U region ($J/U < j_{d1}$) agrees qualitatively with the three-band Kanamori model [28,29] and will not be discussed further. A quantitative comparison is left for future works [16].

Our current interest lies in the Hund's-metal [18] and valence-skipping regimes ($j_{d1} \lesssim J/U \lesssim j_{d2}$). In general, for fixed J/U there is a critical coupling $U = U_c$ where the metal-insulator transition occurs. But as seen in Fig. 4, the U_c of the Hund's metal grows with increased J/U, and when $J/U \to j_{d1}$ it diverges ($U_c \to \infty$). At this point, $J/U = j_{d1}$, the metallicity prevails for any U because the energy cost for charge fluctuations is zero, $U_{\text{eff}}(j_{d1}) = 0$. When entering the valence-skipping regime ($j_{d1} < J/U < j_{d2}$), U_c becomes finite again as a reentrant valence-skipping $d^5 + d^7$ insulator emerges. Yet, approaching the upper boundary $J/U \to j_{d2}$, U_c diverges again. Further increasing J/U rapidly reduces U_c in favor of a valence-split $d^5 + d^{10}$ insulator.

How is then the metal influenced by the change in the ensemble ground state from d^6 to $d^5 + d^7$? In terms of local valences, the single-particle hopping in the metal generates a distribution of adjacent valences. This distribution, however, is strongly dependent on the intra-atomic interaction.

To investigate this, we compute the reduced local many-body density matrix $\hat{\rho}$ [27], and calculate the valence weights ρ_N as traces of $\hat{\rho}$ in every N-electron subspace. The valence distributions ρ_N for the Hund's and valence-skipping metals are shown in Fig. 5, at the points marked out in the phase diagram (Fig. 4). In each case, ρ_N for the corresponding noninteracting metal ($U = 0$) and insulator ($U \to \infty$) are shown for comparison.

The Hund's metal in Fig. 5(a) has an atomiclike valence distribution that is substantially narrower compared to the noninteracting metal. Most of the weight is concentrated in the range $N = 5$–7, with a strong prevalence toward the total average valence $n = 6$. Turning to Fig. 5(b) and the valence-skipping metal, we find the same narrowing down of the distribution, but without any certain valence prevalence.

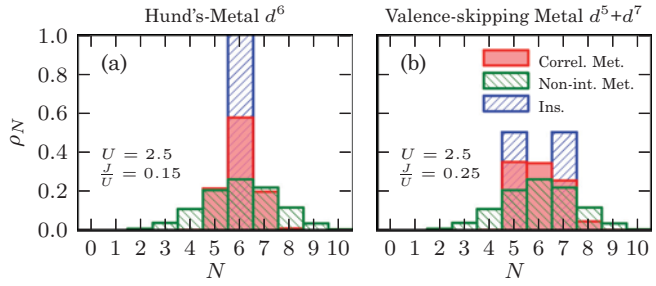

FIG. 5. (Color online) Histograms of valence weights ρ_N as a function of filling N for the points marked in Fig. 4, with $1/\gamma = 1/4$. The correlated metal (red) is shown together with the corresponding $U = 0$ noninteracting metal (green), and the $U \to \infty$ insulator (blue), for (a) the Hund's metal, and (b) the valence-skipping $d^5 + d^7$ metal.

Thus, in comparison to the Hund's metal, there is a substantial reduction of the average d^6 valence. This type of reduction is the hallmark of the anomalous valence fluctuations driven by the effective negative-U in the valence-skipping region.

V. DISCUSSION

We have shown that the local multipole interactions drastically reduce the effective Hubbard repulsion U_{eff} in the d-band, even making it possible to reach negative-U ($U_{\text{eff}} < 0$). Moreover, this multipole reduction is only obtained for four out of ten possible integer d-band fillings, namely d^1, d^4, d^6, and d^9. Admittedly, we have used an oversimplistic model of the d-band. But the valence-skipping active fillings is a fundamental property of the Coulomb interaction, and it applies to the entire class of transition metals.

Experimentally, valence-skipping is most clearly observed when accompanied by charge order and $U_{\text{eff}} < 0$, as in the iron d^4 compounds discussed in the Introduction [4–7], and noble-metal d^9 systems such as $CsAuI_3$ [30]. However, multipole-reduced but positive $U_{\text{eff}} \gtrsim 0$ also generate valence-skipping in terms of polarons at elevated temperatures, $T \gtrsim U_{\text{eff}}$. This type of thermally induced valence-skipping has been used to explain the polaronic conduction in d^6 (La,Ca)CoO_3 [31] and d^4 (La,Ca)MnO_3 [32]. For the d^1 filling, some of the candidate transition-metal complex-oxide compounds are not even thermodynamically stable [1], e.g., $La_2V_2O_7$ phase-separates directly to $LaVO_3$ and $LaVO_4$ ($d^1 \to d^0 + d^2$) [33].

So returning to the propositions of Anderson [2] and Varma [1], we conclude that for multipole-active fillings, the electron interaction can drive valence-skipping even in the absence of lattice relaxation. One such example is $La_{1/2}Ca_{1/2}FeO_3$, which charge-orders to $3(d^{3.5}) \to 2(d^3) + d^5$ [4], while in other cases both multipole interactions and static lattice relaxation combine to give $U_{\text{eff}} < 0$. Note that the valence-skipping phase of the multipole-active fillings is also present for finite crystal fields Δ as long as $\Delta \lesssim U$, as explicitly shown in Appendix A for the case of cubic crystal-field splitting. Strong cubic crystal fields $\Delta_c \gg U$ shift the valence-skipping from d^6 to d^7, as also observed in $YNiO_3$, where the valence-skipping charge order is isolated to the crystal-field-split e_g states, $t_{2g}^6 e_g^1 \to t_{2g}^6 e_g^0 + t_{2g}^6 e_g^2$ [9].

From the Gutzwiller calculations, it is clear that multipole interactions also affect the metallic state. The importance of the metallic valence distribution has been discussed in a recent study of $SrCoO_3$ using the Kanamori interaction [34]. Here a follow-up study also including multipole interactions through the Slater-Condon interaction would be very interesting.

Although valence-skipping is experimentally most evident in charge-ordered compounds, negative-U is also a potential electron-pairing mechanism for superconductivity [12]. Therefore, it is worth noting that the cuprate (d^9: Cu^{2+}), ruthanate (d^4: Ru^{4+}), and iron pnictide and chalcogenide (d^6: Fe^{2+}) superconductors all have multipole-active d-band fillings.

VI. CONCLUSION

To conclude, we have shown that, in the vicinity of the multipole-active fillings d^1, d^4, d^6, and d^9, the multipole part of the Slater-Condon interaction can alone drive valence-skipping $d^n \to d^{n-1} + d^{n+1}$ and negative-U in the degenerate d-band. Furthermore, the valence fluctuations in the valence-skipping metal are drastically different compared to the atomiclike Hund's metal. None of these effects is captured by the Kanamori interaction, due to its lack of anisotropic multipole interactions.

ACKNOWLEDGMENTS

I would like to acknowledge B. Hellsing and M. Granath for a careful reading of the manuscript, and P. Erhart, A. Lichtenstein, S. Biermann, and P. Werner for fruitful discussions. This work was supported by the Mathematics-Physics Platform ($\mathcal{MP}^2$) at the University of Gothenburg, and the Royal and Hvitfeldtska foundation through a visiting stipend for Jonsereds Mansion and Villa Martinsson, where this manuscript was completed. The simulations were performed on resources provided by the Swedish National Infrastructure for Computing (SNIC) at Chalmers Centre for Computational Science and Engineering (C3SE) (Project No. 01-11-297).

APPENDIX A: CRYSTAL FIELDS

In the main text of this article, we employed the locally rotationally invariant model, which enabled direct derivation of analytic expressions for the valence-skipping phase boundaries, j_{d1}, j_{d2}, and Eq. (3). However, this simplification raises the question of whether the valence-skipping phenomenon is of physical relevance for real materials where the local symmetry is lowered by the lattice point group.

To address this issue, we test the robustness of the phases in the atomic ensemble limit in the case of the cubic point group. By combining the local interaction (with $1/\gamma = 1/4$) with a cubic crystal field Δ—lifting the degeneracy of the e_g and t_{2g} irreducible representations of the d-orbitals—the stability of the charge disproportionate phases can be assessed directly; see Fig. 6. Note that for all multipole-active fillings, the valence-skipping phases prevail for $\Delta \leqslant U$.

The robustness of the valence-skipping phases for the multipole-active fillings with respect to a cubic crystal field shows that the valence-skipping phenomenon is relevant for many $3d$ transition-metal systems. The observed importance

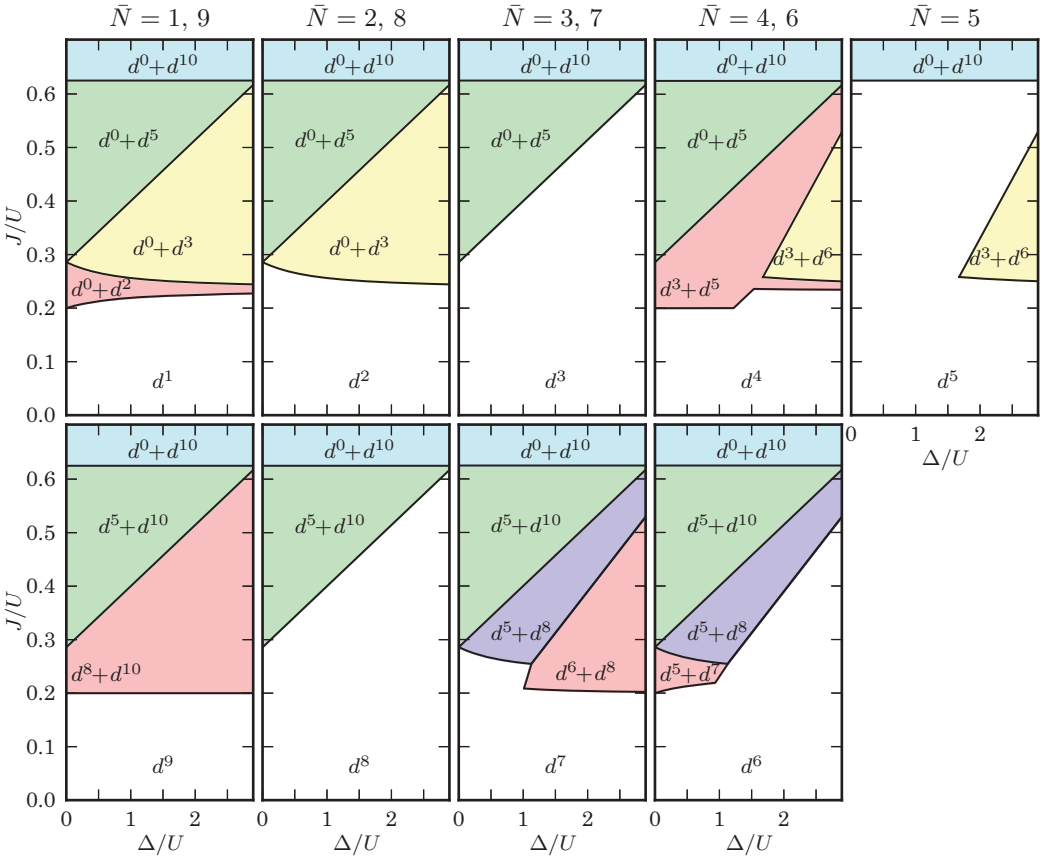

FIG. 6. (Color online) Ensemble phase diagram for finite cubic crystal-field splittings Δ (with $1/\gamma = 1/4$). For all multipole-active fillings d^1, d^4, d^6, and d^9, the valence-skipping $d^{n-1} + d^{n+1}$ is present for $\Delta \leqslant U$. For strong cubic crystal fields $\Delta > U$, all these phases persist except the d^6 phase, which vanishes in favor for the e_g valence-skipping phase emerging for d^7.

of the multipole scattering in reducing U_{eff} could very well turn out to be one of the missing pieces in the unconventional superconductivity puzzle.

We also note that the d^9 valence skipping state turns out to be completely insensitive to the crystal-field strength, see Fig. 6, as also in the $\Delta \to \infty$ limit the resulting effective two-band e_g Hamiltonian displays the same valence-skipping charge disproportionation. This is directly relevant for the cuprate family having very strong cubic crystal fields.

This also leads us to the limit of infinite cubic crystal fields $\Delta \to \infty$. The same type of ensemble analysis can of course be performed using the atomic multiplets of the effective model for an e_g or t_{2g} manifold (for which the Coulomb interaction simplifies to the Kanamori interaction). As the Kanamori interaction has the simple form of Eq. (1), the ground-state multiplets have only two contributions as a function of filling N: (i) a quadratic contribution from the pair interaction $N(N-1)$, and (ii) a piecewise linear "Hund's exchange" contribution from the corresponding $(\hat{Q}^2 - \hat{S}^2)$ term, with a discontinuity at half-filling analogous to the one shown in Fig. 3.

Now, valence-skipping charge disproportionation is only stabilized in the e_g case, in which Hund's exchange stabilizes the valence-skipping $e_g^1 \to e_g^0 + e_g^2$ and $e_g^3 \to e_g^2 + e_g^4$, corresponding to d^7 and d^9, respectively. These valence-skipping phases are present for $\Delta > U$; see Fig. 6. In the t_{2g} case, the same mechanism instead drives a valence-split disproportionation, with combinations of empty and half-filling $(t_{2g}^0 + t_{2g}^3)$ or half-filling and completely filled $(t_{2g}^3 + t_{2g}^6)$; see the yellow phase regions in Fig. 6. For the e_g and t_{2g} effective models, where the Coulomb interaction simplifies to the Kanamori interaction, the interaction parameter constraint for valence phase separation is $U - 3J < 0$. This has been suggested to be the case for the effective e_g model of $YNiO_3$ [9].

APPENDIX B: VALENCE-SPLIT STATES

The observed valence-split states appearing in the phase diagram of both the itinerant and atomic ensemble incarnations of the model call for a small digression. As previously noted, this class of ensemble ground states of multiplets with disparate fillings, e.g., $d^0 + d^5$, is unlikely to occur in real materials, as the low-energy effective model is expected to break down for strong orbital polarizations.

However, in the atomic ensemble limit the valence-split states naturally occur as special cases of binary mixtures of valence states with a fixed average filling n. The particular phase-separated mixtures $d^0 + d^5$ and $d^5 + d^{10}$ turn out to have the lowest possible energy given by $E_{0,5}^{(n)}$ for $n < 5$ and $E_{5,10}^{(n)}$ for $n > 5$, respectively, compared to all other possible configurations in the (green) range of interaction

parameters in Fig. 2. As with any binary phase-separated ensemble state, the split-valence states corresponds to an ensemble with two valence configurations in proportion so as to produce the average filling n. For example, in the nominal d^6 ensemble (with $n = 6$), the corresponding valence-split ensemble ground state has the following proportions: 4/5 parts of d^5 and 1/5 parts of d^{10}, giving the average electron count of $n = 5 \times 4/5 + 10 \times 1/5 = 6$.

The valence-split state is a direct effect of the Kanamori part of the local interaction. It can be understood directly in the limit of zero multipole interaction $1/\gamma = 0$, where the valence-split state appears for $J/U > 1/3$ (i.e., when $U - 3J < 0$). The energy contributions to the local interaction can then be inferred directly from Fig. 3. The prefactor $U - 3J$ of the density-density contribution $N(N-1)$ is now negative, causing the multiplet energies to be concave in both ranges $0 \leqslant N \leqslant 5$ and $5 \leqslant N \leqslant 10$. However, it is the $Q^2 - S^2$ term in Eq. (1) that divides the interval $N \in [0,10]$ into two pieces, due to its discontinuous slope at $N = 5$. The resulting form of the ground-state multiplet energies gives directly the $d^0 + d^5$ and $d^5 + d^{10}$ configurations as the ensemble ground states in the two regimes $n < 5$ and $n > 5$, respectively.

[1] C. M. Varma, Phys. Rev. Lett. **61**, 2713 (1988).
[2] P. W. Anderson, Phys. Rev. Lett. **34**, 953 (1975).
[3] W. A. Harrison, Phys. Rev. B **74**, 245128 (2006).
[4] Y.-Q. Liang, N.-l. Di, and Z.-h. Cheng, Phys. Rev. B **72**, 134416 (2005).
[5] J. Matsuno, T. Mizokawa, A. Fujimori, Y. Takeda, S. Kawasaki, and M. Takano, Phys. Rev. B **66**, 193103 (2002).
[6] J. Matsuno, T. Mizokawa, A. Fujimori, K. Mamiya, Y. Takeda, S. Kawasaki, and M. Takano, Phys. Rev. B **60**, 4605 (1999).
[7] K. Kuzushita, S. Morimoto, S. Nasu, and S. Nakamura, J. Phys. Soc. Jpn. **69**, 2767 (2000).
[8] H. Katayama-Yoshida and A. Zunger, Phys. Rev. Lett. **55**, 1618 (1985).
[9] I. I. Mazin, D. I. Khomskii, R. Lengsdorf, J. A. Alonso, W. G. Marshall, R. M. Ibberson, A. Podlesnyak, M. J. Martínez-Lope, and M. M. Abd-Elmeguid, Phys. Rev. Lett. **98**, 176406 (2007).
[10] I. Hase and T. Yanagisawa, Phys. Rev. B **76**, 174103 (2007).
[11] A. S. Moskvin, Phys. Rev. B **79**, 115102 (2009).
[12] R. Micnas, J. Ranninger, and S. Robaszkiewicz, Rev. Mod. Phys. **62**, 113 (1990).
[13] L. Vaugier, H. Jiang, and S. Biermann, Phys. Rev. B **86**, 165105 (2012).
[14] Z. Rudzikas, *Theoretical Atomic Spectroscopy*, Cambridge Monographs on Atomic, Molecular and Chemical Physics (Cambridge University Press, Cambridge, 2007).
[15] B. R. Judd and G. M. S. Lister, J. Phys. B **17**, 3637 (1984).
[16] H. U. R. Strand, N. Lanatà, M. Granath, and B. Hellsing (unpublished).
[17] T. Mizokawa and A. Fujimori, Phys. Rev. B **51**, 12880 (1995).
[18] A. Georges, L. d. Medici, and J. Mravlje, Annu. Rev. Condens. Matter Phys. **4**, 137 (2013).
[19] D. van der Marel and G. A. Sawatzky, Phys. Rev. B **37**, 10674 (1988).
[20] F. M. F. de Groot, J. C. Fuggle, B. T. Thole, and G. A. Sawatzky, Phys. Rev. B **42**, 5459 (1990).
[21] G. Racah, Phys. Rev. **62**, 438 (1942).
[22] E. U. Condon and G. H. Shortley, *The Theory of Atomic Spectra* (Cambridge University Press, Cambridge, 1959).
[23] M. Fabrizio, Phys. Rev. B **76**, 165110 (2007).
[24] N. Lanatà, P. Barone, and M. Fabrizio, Phys. Rev. B **78**, 155127 (2008).
[25] N. Lanatà, H. U. R. Strand, X. Dai, and B. Hellsing, Phys. Rev. B **85**, 035133 (2012).
[26] L. Huang, L. Du, and X. Dai, Phys. Rev. B **86**, 035150 (2012).
[27] L. Amico, R. Fazio, A. Osterloh, and V. Vedral, Rev. Mod. Phys. **80**, 517 (2008).
[28] L. de' Medici, J. Mravlje, and A. Georges, Phys. Rev. Lett. **107**, 256401 (2011).
[29] L. de' Medici, Phys. Rev. B **83**, 205112 (2011).
[30] S. S. Hafner, N. Kojima, J. Stanek, and L. Zhang, Phys. Lett. A **192**, 385 (1994).
[31] S. R. Sehlin, H. U. Anderson, and D. M. Sparlin, Phys. Rev. B **52**, 11681 (1995).
[32] M. F. Hundley and J. J. Neumeier, Phys. Rev. B **55**, 11511 (1997).
[33] H. Yokokawa, N. Sakai, T. Kawada, and M. Dokiya, Solid State Ion. **52**, 43 (1992).
[34] J. Kuneš, V. Křápek, N. Parragh, G. Sangiovanni, A. Toschi, and A. V. Kozhevnikov, Phys. Rev. Lett. **109**, 117206 (2012).